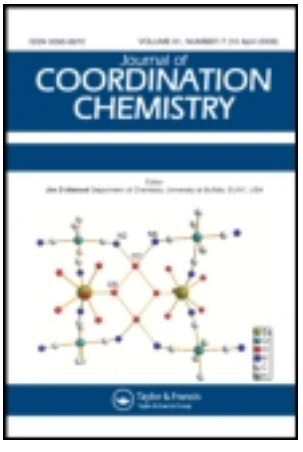

Journal of Coordination Chemistry
Publication details, including instructions for authors and subscription information:
http://www.tandfonline.com/loi/gcoo20

# Two oxovanadium complexes incorporating thiosemicarbazones: synthesis, characterization, and DNA-binding studies

Jia-Zheng Lu [a], Yi-Fan Du [a], Hai-Wei Guo [a], Jing Jiang [a], Xian-Dong Zeng [a] & Lin-Quan Zang [a]

[a] The School of Pharmacy, Guangdong Pharmaceutical University, Guangzhou 510006, P.R. China

Published online: 08 Apr 2011.

To cite this article: Jia-Zheng Lu, Yi-Fan Du, Hai-Wei Guo, Jing Jiang, Xian-Dong Zeng & Lin-Quan Zang (2011) Two oxovanadium complexes incorporating thiosemicarbazones: synthesis, characterization, and DNA-binding studies, Journal of Coordination Chemistry, 64:7, 1229-1239

To link to this article: http://dx.doi.org/10.1080/00958972.2011.565754

*Journal of Coordination Chemistry*
Vol. 64, No. 7, 10 April 2011, 1229–1239

Taylor & Francis
Taylor & Francis Group

# Two oxovanadium complexes incorporating thiosemicarbazones: synthesis, characterization, and DNA-binding studies

JIA-ZHENG LU*, YI-FAN DU, HAI-WEI GUO, JING JIANG, XIAN-DONG ZENG and LIN-QUAN ZANG

The School of Pharmacy, Guangdong Pharmaceutical University, Guangzhou 510006, P.R. China

(*Received 3 May 2010; in final form 1 February 2011*)

An oxovanadium complex [VO(satsc)(phen)] (**1**) (satsc = salicylaldehyde thiosemicarbazone, phen = phenanthroline) and its derivative [VO(3,5-dibrsatsc)(phen)] (**2**) (3,5-dibrsatsc = 3, 5-dibromosalicylaldehyde thiosemicarbazone) have been synthesized and characterized by elemental analysis, infrared, electrospray-mass spectra, $^1$H NMR, and magnetic susceptibility measurements. The DNA-binding behaviors of these complexes with calf-thymus DNA (CT-DNA) were investigated by UV-Vis absorption titration, fluorescence spectra, viscosity measurements, thermal denaturation, and circular dichroism. Both **1** and **2** bind to CT-DNA by intercalation and **1** exhibits much stronger binding affinity to CT-DNA than **2**.

*Keywords*: Synthesis; Oxovanadium; Thiosemicarbazone; DNA; Thermal denaturation



## 1. Introduction

Transition metal complexes have been widely employed in studies of DNA [1, 2]. In particular, complexes with polyaromatic ligands have been used as DNA-structural probes, DNA-dependent electron transfer, sequence-specific cleaving agents, and potential anti-cancer drugs [3–5].

Complexes having metal ions with strong Lewis acidity could show cleavage of DNA, modeling the activity of restriction enzymes [3, 4]. As a trace biocompatible element which exists at the active site of several enzymes, derivatives of vanadium have been reported to display biological effects including anti-tumor, anti-microbial, anti-hyperlipidemia, anti-hypertension, anti-obesity, enhancement of oxygen affinity of hemoglobin and myoglobin, insulin-enhancing effects, etc. [6–12]. Much effort has been done for vanadyl species coordinated to organic ligands on insulin mimetic effects in hopes of developing vanadodrugs [13]. Vanadium also takes part in various DNA-maintenance reactions and thereby prevents genomic instability which otherwise leads to cancer [14, 15]. Understanding of how these molecules bind to DNA will be useful in designing new drugs and reactive probes and diagnostic reagents. Some symmetrical

*Corresponding author. Email: lujia6812@163.com

*Journal of Coordination Chemistry*
ISSN 0095-8972 print/ISSN 1029-0389 online 
DOI: 10.1080/00958972.2011.565754

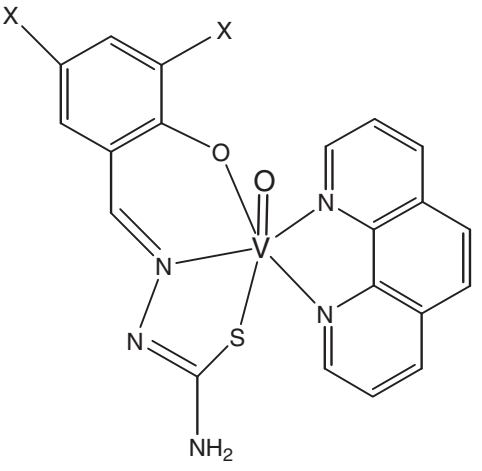


Scheme 1. Structures of [VO(satsc)(phen)] (**1**), X = H and [VO(3,5-dibrsatsc)(phen)] (**2**), X = Br.

vanadyl-enrofloxacin and N-salicylidene-S-methyl dithiocarbazate oxovanadium complexes of phenanthroline have been reported for the interactions with calf-thymus DNA (CT-DNA) [14–16]. A vanadyl complex incorporating 3,4-dihydroxybenzylidene thiosemicarbazide has also been studied for eukaryotic DNA degradation [16]. Thus, vanadyl complexes bearing thiosemicarbazones have potential effects on DNA, which may be related with the fact that thiosemicarbazones can bind to the nitrogen base of DNA, hinder or block base replication, and create lesions in DNA strands by oxidative rupture [17]. However, the mechanisms by which they interact with DNA have not been clearly elucidated [16–20]. In this regard, we center our interest on the interaction of thiosemicarbazone oxovanadium complexes with DNA and try to investigate their possible mechanism of interaction with DNA. Here, an oxovanadium complex [VO(satsc)(phen)] (**1**) (satsc = salicylaldehyde thiosemicarbazone, phen = phenanthroline) and its derivative [VO(3,5-dibrsatsc)(phen)] (**2**) (3,5-dibrsatsc = 3,5-dibromosalicylaldehyde thiosemicarbazone, scheme 1) have been synthesized and characterized by elemental analysis, infrared (IR), electrospray-mass spectra (ES-MS), $^1$H NMR, UV-Vis, and magnetic susceptibility measurements. The DNA-binding behaviors of these two complexes with CT-DNA were investigated using UV-Vis absorption titration, fluorescence spectra, viscosity measurements, thermal denaturation, and circular dichroism (CD).

## 2. Experimental

### 2.1. *Materials and methods*

$VO(acac)_2$ (acac = acetylacetonate) and 1,10-phenanthroline (phen) were commercially available and used as received. CT-DNA was obtained from Sigma Company. Tris buffer (Tris = Tris(hydroxyl-methyl) aminomethane) containing 5 mmol $L^{-1}$ Tris-HCl, 50 mmol $L^{-1}$ NaCl (pH = 7.2) was used for absorption titration, fluorescence emission,

viscosity measurements, and CD. A phosphoric acid buffer containing 1.5 mmol $L^{-1}$ $Na_2HPO_4$, 0.5 mmol $L^{-1}$ $NaH_2PO_4$, and 0.25 mmol $L^{-1}$ $Na_2H_2EDTA$ ($H_4EDTA$ = *N,N′*-ethane-1,2-diylbis[*N*-(carboxymethyl)glycine]) (pH = 7.0) was used for thermal denaturation. A solution of CT-DNA in Tris buffer gave a ratio of UV absorbance at 260 and 280 nm of 1.8–1.9 : 1, indicating that the DNA was sufficiently free of protein [18]. The DNA concentration per nucleotide was determined by absorption spectroscopy using the molar absorption coefficient (6600 $(mol\,L^{-1})^{-1}\,cm^{-1}$) at 260 nm [19].

### 2.2. *Physical measurements*

Microanalysis (C, H, and N) was carried out with a Perkin-Elmer 240Q elemental analyzer. ES-MS were recorded on a LCQ system (Finnigan MAT, USA) using methanol as mobile phase. $^1H$ NMR spectra were recorded on a Varian-500 spectrometer. All chemical shifts are given relative to tetramethylsilane (TMS). IR spectra were recorded on a Bomen FTIR model MB102 instrument using KBr pellets. UV-Vis spectra were recorded on a Shimadzu UV-3101 PC spectrophotometer at room temperature. Emission spectra were recorded on a Perkin-Elmer Lambda 55 spectrofluorophotometer. Magnetic susceptibility measurements were recorded on a MPMSXL-7(Quantum Design, USA) at room temperature. CD spectra were recorded on a JASCO-J810 spectrometer.

### 2.3. *DNA-binding studies*

Absorption titration of the oxovanadium complex in Tris buffer was performed by using a fixed concentration of the oxovanadium complex (20 μmol $L^{-1}$) to which DNA stock solution was added. Oxovanadium–DNA solution was allowed to incubate for 3 min before the absorption spectra were recorded. In order to further elucidate the binding strength of the complex, the intrinsic binding constant $K_b$ with CT-DNA was obtained by monitoring the change in the absorbance of the ligand-transfer band with increasing amounts of DNA. The intrinsic binding constant $K_b$ of the complex to DNA was calculated using the following equation [20]:

$$\frac{[DNA]}{\varepsilon_a - \varepsilon_f} = \frac{[DNA]}{\varepsilon_a - \varepsilon_f} + \frac{1}{K_b(\varepsilon_b - \varepsilon_f)},$$

where $[DNA]$ is the concentration of DNA in base pairs; $\varepsilon_a$, $\varepsilon_f$ and $\varepsilon_b$ refer to the corresponding apparent absorption coefficient $A_{obsd}$/[Vanadium], the extinction coefficient for the free oxovanadium complex, and the extinction coefficient for the oxovanadium complex in the fully bound form, respectively. In plots of $[DNA]/(\varepsilon_a - \varepsilon_f)$ *versus* $[DNA]$, $K_b$ is obtained as the ratio of the slope to the intercept.

Viscosity measurements were carried out using an Ubbelohde viscometer maintained at 28 ± 0.1°C in a thermostatic bath. Flow time was measured with a digital stopwatch and each sample was measured five times to obtain the average flow time. Data were presented as $(\eta/\eta_0)^{1/3}$ *versus* binding ratio [21], where $\eta$ is the viscosity of DNA in the presence of complexes while $\eta_0$ is the viscosity of DNA alone.

Thermal denaturation studies were carried out with a Shimadzu UV-3101 PC spectrophotometer equipped with a Peltier temperature-controlling

programmer (±0.1°C). The melting curves were obtained by measuring the absorbance at 260 nm for the solutions of CT-DNA (100 μmol $L^{-1}$) in the absence and presence of different concentrations of the oxovanadium complexes as a function of temperature. The temperature was scanned from 40°C to 92°C at a speed of 1°C $min^{-1}$. The melting temperature ($T_m$) was taken as the midpoint of the hyperchromic transition.

The CD spectra of **1** and **2** in the absence and presence of CT-DNA were performed on a JASCO-J810 spectrometer using a fixed concentration of the oxovanadium complex [V] = 10 μmol $L^{-1}$ and [DNA] = 130 μmol $L^{-1}$, respectively. The spectra were recorded at 25°C after samples had been incubated with CT-DNA for 24 h at 37°C.



### 2.4. *Synthesis and characterization*

Salicylaldehyde thiosemicarbazone (satsc) and 3,5-dibromosalicylaldehyde thiosemicarbazone (3,5-dibrsatsc) were prepared with a method similar to that described earlier [15, 22, 23]. An equimolar methanolic solution of desired thiosemicarbazide (0.0182 g, 10 mmol) and corresponding salicylaldehyde (0.0244 g, 10 mmol) or 3,5-dibromosalicylaldehyde (0.0560 g, 10 mmol) was refluxed for 3 h and then the precipitates were filtered off, washed with methanol, and dried under vacuum. The products were recrystallized in ethanol. Satsc: white solid. Yield: 80%. $^1$H NMR (DMSO-$d_6$, 500 MHz) $\delta$: 11.34 (s, 1 H, $J$ = 10.8 Hz), 9.88 (s, 1 H, $J$ = 9.2 Hz), 7.21 (t, 1 H, $J$ = 7.1 Hz), 6.86 (d, 1 H, $J$ = 7.7 Hz), 6.81 (d, 1 H, $J$ = 7.6 Hz), 6.79 (t, 1 H, $J$ = 7.6 Hz). ES-MS ($CH_3OH$): $m/z$ 196.0 ($[M+H]^+$). IR (KBr disk): $\nu$($cm^{-1}$) = 3443, 3319, 3173, 1603, 1537, 1463, 1265, 829, 752. $\lambda_{max}$, nm ($\varepsilon$, $(mol\,L^{-1})^{-1}\,cm^{-1}$) in DMSO: 340 (26310). 3,5-dibrsatsc: white solid. Yield: 85%. $^1$H NMR (DMSO-$d_6$, 500 MHz) $\delta$: 11.54 (s, 1 H, $J$ = 11.4 Hz), 9.97 (s, 1 H, $J$ = 9.3 Hz), 8.16 (s, 1 H, $J$ = 8.0 Hz), 7.75 (s, 1 H, $J$ = 7.8 Hz). ES-MS ($CH_3OH$): $m/z$ 353.8 ($M^+$). IR (KBr disk): $\nu$($cm^{-1}$) = 3467, 3356, 3013, 1614, 1535, 1448, 1287, 859, 714. $\lambda_{max}$, nm ($\varepsilon$, $(mol\,L^{-1})^{-1}\,cm^{-1}$) in DMSO: 346 (18655).

**2.4.1. [VO(satsc)(phen)].** A mixture of satsc (0.0731 g, 0.375 mmol) and phen·$H_2O$ (0.0743 g, 0.375 mmol) in absolute alcohol (20 $cm^3$) was heated at 72°C under argon for 30 min. After dissolution, $VO(acac)_2$ (0.1000 g, 0.375 mmol) was added and the brown-red precipitate was formed immediately. This suspension was kept stirring under reflux for about 3.5 h and then the colored solid formed was filtered from the hot solution, washed with mixed ethanol and ether three times, and dried under vacuum. Yield: 90%. Anal. Found (%): C, 54.14; H, 3.39; N, 15.82. Calcd for $C_{20}H_{15}N_5O_2SV$ (%): C, 54.55; H, 3.44; N, 15.92. $^1$H NMR (DMSO-$d_6$, 500 MHz) $\delta$: 9.11 (d, 2 H, $J$ = 8.9 Hz), 8.51 (t, 2 H, $J$ = 9.5 Hz), 7.97 (d, 2 H, $J$ = 7.5 Hz), 7.78 (d, 2 H, $J$ = 7.8 Hz), 7.22 (t, 1 H, $J$ = 3.9 Hz), 6.86 (d, 1 H, $J$ = 7.7 Hz), 6.82 (d, 1 H, $J$ = 7.7 Hz), 6.77 (t, 1 H, $J$ = 7.6 Hz), 6.75 (t, 1 H, $J$ = 7.6 Hz). ES-MS ($CH_3OH$): $m/z$ 441.1 ($[M+H]^+$). IR (KBr disk): $\nu$($cm^{-1}$) =3284, 1625, 1603, 1441, 940, 767, 598. $\lambda_{max}$, nm ($\varepsilon$, $(mol\,L^{-1})^{-1}\,cm^{-1}$) in DMSO: 265 (41770), 340 (15255), 383 (6525), 760 (20), 797 (20). Magnetic moment: $\mu_{eff}$: 1.64 BM.

**2.4.2. [VO(3,5-dibrsatsc)(phen)].** This complex was synthesized with the same method described for **1**. Yield: 89%. Anal. Found (%): C, 40.05; H, 2.15; N, 11.44. Calcd for $C_{20}H_{13}N_5O_2SBr_2V$ (%): C, 40.13; H, 2.19; N, 11.71. $^1$H NMR (DMSO-$d_6$, 500 MHz)

$\delta$: 9.11 (d, 2 H, $J = 8.8$ Hz), 8.51 (d, 2 H, $J = 8.1$ Hz), 8.01 (s, 1 H, $J = 7.7$ Hz), 7.79 (d, 2 H, $J = 7.8$ Hz), 7.78 (d, 2 H, $J = 7.8$ Hz). ES-MS ($CH_3OH$): $m/z$ 598.9 ($M^+$). IR (KBr disk): $\nu(cm^{-1}) = 3289$, 1624, 1598, 1439, 965, 769, 624. $\lambda_{max}$, nm ($\varepsilon$, $(mol\,L^{-1})^{-1}\,cm^{-1}$) in DMSO: 264 (41015), 347 (10975), 400 (7815), 786 (20). Magnetic moment: $\mu_{eff}$: 1.67 BM.

## 3. Results and discussion

### 3.1. *Complex characterization*

Oxovanadium(IV) complexes, [VO(satsc)(phen)] (**1**) (satsc = salicylaldehyde thiosemicarbazone, phen = phenanthroline) and [VO(3,5-dibrsatsc)(phen)] (**2**) (3,5-dibrsatsc = 3,5-dibromosalicylaldehyde thiosemicarbazone) are prepared in high yield when vanadyl acetylacetonate is reacted with the ligands in ethanol.

To study the binding mode of the ligand to vanadium, IR spectra of the free ligands were compared with the spectra of the vanadium complexes. Selected IR data for complexes and free ligands are given in table 1. For the ligands, characteristic stretching vibrations appear at 859 and/or 829 $cm^{-1}$ corresponding to C=S. A strong band in the free ligands at 1614 or 1603 $cm^{-1}$ is characteristic of the imine (C=N) [24, 25]. In spectra of the complexes, $\nu$(C=N) showed red shifts to 1625 and 1624 $cm^{-1}$, indicating coordination of nitrogen to vanadium (table 1; [26, 27]). Medium intensity band at 3467 and 3443 $cm^{-1}$ in free ligands due to $\nu_{(OH)}$ were absent in the complexes, indicating deprotonation prior to coordination [25, 27]. The complexes exhibit characteristic $\nu$(V=O) at 965 and 940 $cm^{-1}$, and $\nu$(V–O) at 624 and 598 $cm^{-1}$ for **1** and **2**, respectively.

$^1$H NMR spectra of **1** and **2** are in excellent agreement with the proposed structures. Chemical shifts of the phenolic hydroxy protons of 11.34 and 11.54 ppm, and amino protons linking directly to the imine groups of 9.88 and 9.97 ppm for free ligands are not observed in **1** and **2**, affirming that the ligands are coordinated.

Electronic spectra of the complexes and ligands are shown in figure 1. The complexes show an intense band at 265 nm assignable to $\pi$–$\pi^*$ transitions of aromatic rings of phenanthroline [15, 20, 28]. A medium band is observed near 400 nm, attributed to a ligand-to-metal charge-transfer transition (LMCT) from a p-orbital on the ligand oxygen to the empty d-orbital of vanadium [29]. The remaining bands in the UV-region (320–350 nm) are assignable to intraligand transitions of the Schiff base [15, 26, 28]. Five- and six-coordinate complexes of oxovanadium(IV) are usually square pyramidal/trigonal bipyramidal and distorted octahedral, respectively [29]. From the above obtained spectral data, the Schiff bases bond through phenolate oxygen, imine nitrogen,

Table 1. Selected IR data for complexes and ligands $\nu$ ($cm^{-1}$).

| Compound | $\nu$(C=S) | $\nu$(C–S) | $\nu$(O–H) | $\nu$(C=N) | $\nu$(V=O) | $\nu$(V–O) | $\nu$(N–H) |
|---|---|---|---|---|---|---|---|
| Vo(satsc)(phen) | – | 769 | – | 1625 | 965 | 624 | 3289 |
| *S*atsc | 859 | – | 3467 | 1614 | – | – | 3356 |
| Vo(3,5-dibrsatsc)(phen) | – | 767 | – | 1624 | 940 | 598 | 3284 |
| 3,5-dibrsatsc | 829 | – | 3443 | 1603 | – | – | 3319 |

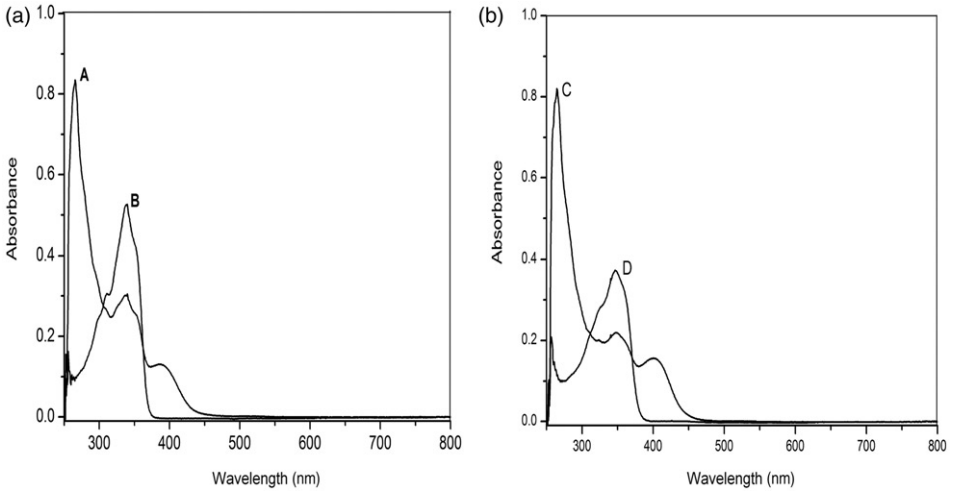


Figure 1. Absorption spectra of (a) VO(satsc)(phen) (A) and its ligand salsem (B) and (b) VO(3,5-dibrsatsc)(phen) (C) and its ligand 3,5-dibrsatsc (D).



and thiolate sulfur leaving the thiomethyl as a pendant group. This implies that **1** and **2** are square pyramidal [15, 29, 30].

The complexes are one-electron paramagnetic giving a magnetic moment value of ~1.6 BM at room temperature, also confirming that the vanadium complexes are V (IV), with $d^1$ configuration [15, 30].

Assignments of the two complexes were made on the basis of elemental analyses and mass spectral data, confirming the proposed structures. The molecular ion peaks of complexes at $m/z$ 441.1 and 598.9 for **1** and **2**, respectively, were obtained by ESI-MS.

### 3.2. *DNA-binding studies*

**3.2.1. Electronic absorption titration.** The binding strength of metallointercalators to DNA is expected to depend on the size and electron density of interacting aromatic rings as well as the combined effect of hydrophobic and hydrophilic interactions [31]. Flatness of the coordinated aromatic rings of the intercalating ligand and additional stabilization by the cooperativity between stacking, hydrogen–bonding, and electrostatic interactions will also affect the DNA-binding affinity.

The electronic absorption spectra of **1** and **2** in the absence and presence of CT-DNA are shown in figure 2. Significant hypochromism but trivial bathochromism were observed for both complexes at 250–290 nm, which is attributed to $\pi \rightarrow \pi^*$. The hypochromicity and bathochromic shift are 38.3% and 4 nm for **1** and 21.6% and 0.5 nm for **2**, respectively. According to previous results [32], we believe that **1** and **2** most likely bind with DNA through a stacking interaction between the aromatic chromophore of the ligands and the base pairs of DNA.

In order to further elucidate the binding strength of these complexes with DNA, the intrinsic binding constant $K_b$ was calculated by monitoring the changes of absorbance in the ligand-transfer bands with the increasing amounts of CT-DNA. The intrinsic

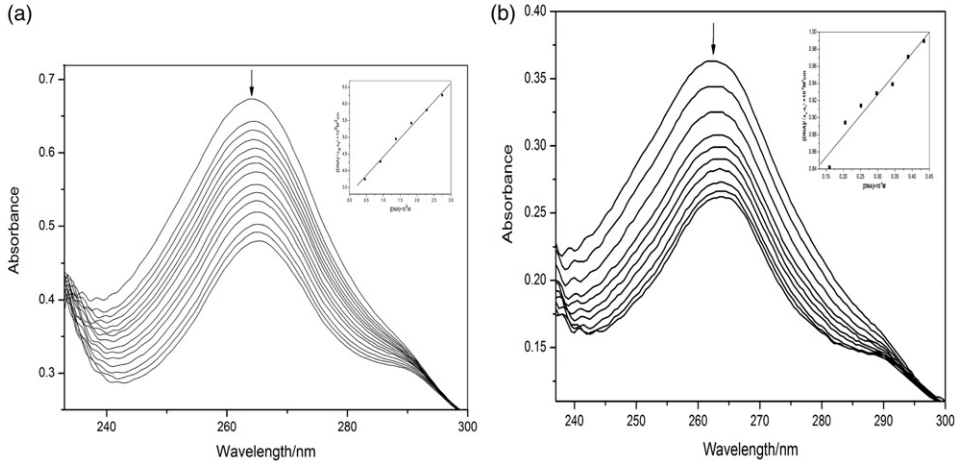


Figure 2. Absorption spectra in Tris-HCl buffer upon increasing the amounts of CT-DNA in the presence of **1** (a) and **2** (b). [V] = 20 μM. Arrow shows the absorbance changing with increase of DNA concentration. Inset: plots of [DNA]/($\varepsilon_a - \varepsilon_f$) *vs.* [DNA] for titration of oxovanadium complexes with CT-DNA.



binding constant $K_b$ obtained for **1** and **2** were $3.2 \times 10^4$ and $2.7 \times 10^4$, respectively, implying that both complexes strongly interact with DNA. Compared with **1**, complex **2** exhibits lower binding strength to double-helical DNA, due to two bromides on the 3- and 5-positions of the aromatic chromophore of salicylaldehyde thiosemicarbazone. Because of their electron-withdrawing effects, the electron density of the aromatic chromophore of thiosemicarbazone which may intercalate into base pairs of CT-DNA in **2** will be altered, changing the stacking interaction between the aromatic chromophore of **2** and the base pairs of DNA and, concomitantly, the intrinsic binding constants $K_b$. This indicates that the electronic effects of the substituents introduced on the aromatic chromophore of the ligands may affect the binding affinity of a complex to DNA.

**3.2.2. Fluorescence spectroscopic studies.** The emission spectra of **1** and **2** in the absence and presence of CT-DNA are shown in figure 3; fixed amounts (20 μmol $L^{-1}$) of **1** and **2** were titrated with increasing amounts of CT-DNA. In the absence and presence of CT-DNA, **1** and **2** exhibit luminescence in Tris buffer, with a maxima appearing at 446 and 465 nm, respectively. Upon addition of CT-DNA, the emission intensities for **1** and **2** grow to around 0.21 and 0.15 times larger than that of **1** and **2** in the absence of CT-DNA and saturates at a [DNA]/[V] ratio of 20 : 1. This implies that both complexes intercalate into the base pairs of DNA and are protected by DNA efficiently, since the hydrophobic environment provided by DNA can protect them from the accessibility of water and thus prolong the luminescence, increasing the emission intensity [33]. In addition, **1** interacts with DNA more strongly than **2**, consistent with the absorption spectra results.

**3.2.3. Viscosity measurements.** To further explore the binding of **1** and **2** to CT-DNA, viscosity measurements were carried out on CT-DNA by changing the concentration of

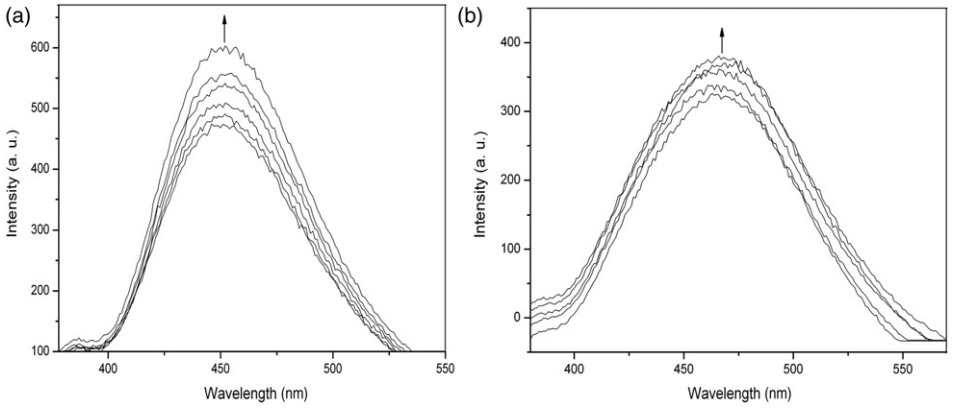


Figure 3. Emission spectra of **1** (a) and **2** (b) in Tris-HCl buffer in the absence and presence of CT-DNA. [V] = 20 μmol $L^{-1}$. Arrows show the intensity changes upon increase of DNA concentration. $\lambda_{exc} = 341$ and 350 nm for **1** and **2**, respectively.

the complex. In the absence of X-ray structural data, viscosity measurements are arguably the most critical test of intercalation and provide the most definitive means of inferring the binding mode of DNA in solution [34–36]. Intercalation results in lengthening the DNA helix as the base pairs are pushed apart to accommodate the bound ligand, leading to an increase in DNA viscosity. In contrast, a partial, non-classical intercalation of the ligand could bend (or kink) the DNA helix reducing its effective length and, concomitantly, its viscosity. In addition, the viscosity of DNA will not change when outside binding or groove-binding appears [37, 38]. The effects of **1** and **2** on the viscosity of CT-DNA are shown in figure 4; upon increasing the amounts of **1** and **2**, the relative viscosity of DNA increases steadily, supporting the conclusion that **1** and **2** interact with CT-DNA by intercalation.

**3.2.4. Thermal denaturation studies.** Melting of DNA can be used to distinguish binding modes between molecules which bind *via* intercalation and those which bind externally. Thermal behaviors of DNA in the presence of compounds can give insight into their conformational changes when the temperature is raised and offer information about the extent of interaction of the compounds with DNA. As the temperature in the solution is increased, the double-stranded DNA will gradually dissociate to single strands and generate a hyperchromic effect on absorption spectra of DNA bases. The melting temperature $T_m$, which is defined as the temperature where half of the total base pairs are unbound, is determined from the thermal denaturation curves of DNA by monitoring the changes of absorption spectra of DNA bases ($\lambda = 260$ nm). Intercalative binding occurs when $T_m$ is considerably increased [39].

The melting curves of CT-DNA in the absence and presence of **1** and **2** are illustrated in figure 5. $T_m$ of CT-DNA alone is $67.1 \pm 0.2$°C and $T_m$ of **1** and **2** observed are $75.0 \pm 0.2$°C and $70.2 \pm 0.2$°C, respectively. The large increase of $T_m$ ($\Delta T_m = 7.9$°C) in the presence of **1** and moderate increases of $T_m$ ($\Delta T_m = 3.1$°C) in the presence of **2** are comparable to that observed for classical intercalators, giving support to their binding with DNA by intercalation [40–43]. In addition, compared with **2**, complex **1** possesses

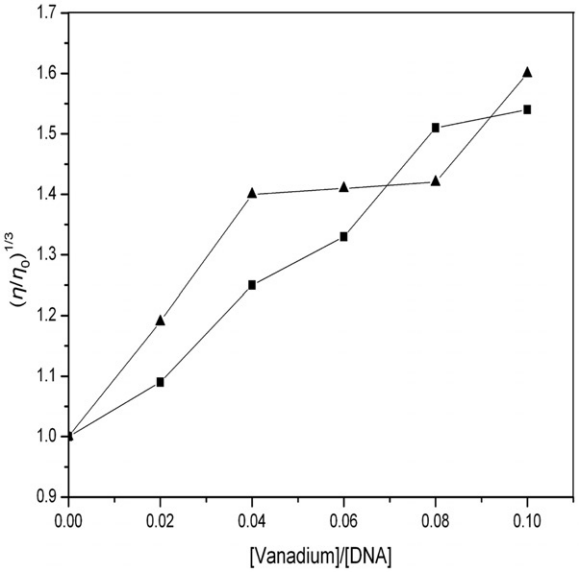


Figure 4. Effects of increasing concentration of **1** (■) and **2** (▲) on the relative viscosity of CT-DNA at $28 \pm 0.1$°C. [DNA] = 0.2 mmol $L^{-1}$.

a larger $\Delta T_m$, indicating that **1** exhibits larger binding strength when interacting with DNA, in conformity with that obtained from electronic absorption titration.

**3.2.5. CD studies.** CD spectra play an important role in the study of the interaction between complexes and DNA as CD spectra are very sensitive to the binding modes of small molecules to DNA. Figure 6 shows CD spectra of **1** (a) and **2** (b) in the absence and in the presence of CT-DNA. A transparent conservative bisignal CD band can be observed for both complexes. Both **1** and **2** exhibit a negative peak centered at 246 nm and a positive peak at 275 nm, which results from interaction between the transition moments of the complexes and chirally arranged DNA base transitions [43–45]. A vanadyl-enrofloxacin complex, $VO(erx)_2(H_2O)$, exhibits a positive peak appearing at 274 nm and a negative peak appearing at 246 nm [46]. The CD spectra of **1** and **2** are consistent with the previous report.

## 4. Conclusion

Oxovanadium complexes [VO(satsc)(phen)] (**1**) (satsc = salicylaldehyde thiosemicarbazone, phen = phenanthroline) and [VO(3,5-dibrsatsc)(phen)] (**2**) (3,5-dibrsatsc = 3, 5-dibromosalicylaldehyde thiosemicarbazone) have been synthesized and characterized. The DNA-binding behaviors of these complexes with CT-DNA were investigated using UV-Vis absorption titration, fluorescence spectra, viscosity measurements, thermal denaturation, and CD. The experimental results show that **1** and **2** bind to CT-DNA by intercalation and **1** exhibits stronger binding affinity to CT-DNA than **2**.

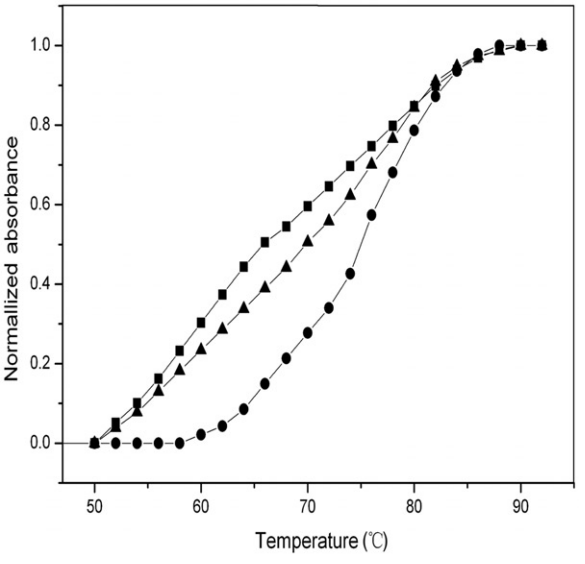


Figure 5. Thermal denaturation of CT-DNA in the absence (■) and presence of **1** (●) and **2** (▲), $[V] = 20\,\mu mol\,L^{-1}$, $[DNA] = 100\,\mu mol\,L^{-1}$.

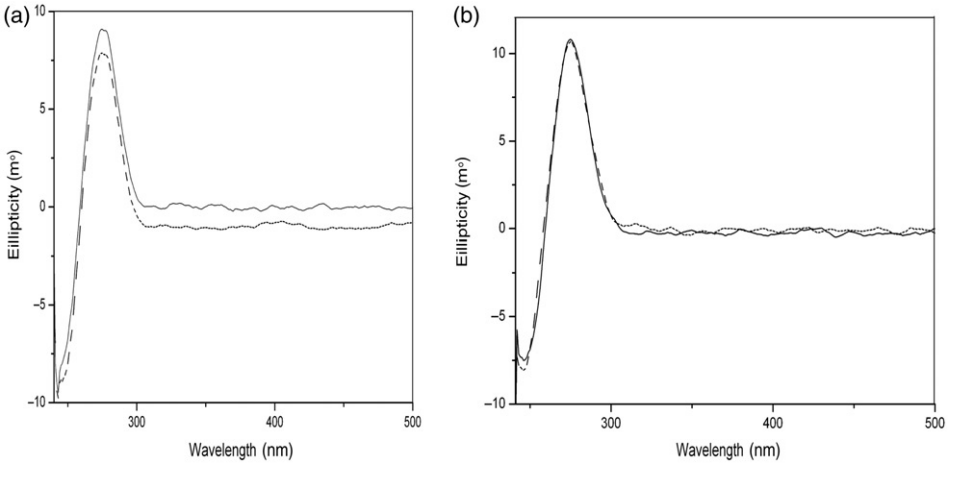


Figure 6. Induced CD spectra of **1** (a) and **2** (b) in the absence (···) and presence (—) of CT-DNA, $[V] = 10\,\mu mol\,L^{-1}$, $[DNA] = 130\,\mu mol\,L^{-1}$. Spectra were recorded at 25°C after samples had been incubated with CT DNA for 24 h at 37°C.

## Acknowledgments

The research was supported by National Natural Science Foundation of China, the National Education Ministry Key Research Project of China (208105), the Scientific Foundation of Zhongshan (2009H018), and the Teacher Culture Foundation of Guangdong Pharmaceutical University (2008) and (43540119).

## References


[1] L.-N. Ji, X.-H. Zou, J.-G. Liu. *Coord. Chem. Rev.*, **216–217**, 513 (2001).
[2] N.A.P. Kane-Maguire, J.F. Wheeler. *Coord. Chem. Rev.*, **211**, 145 (2001).
[3] P. Sangamesh, N. Vinod, K. Ajaykumar, K. Udaykumar, B. Gangadhar, B. Prema. *J. Coord. Chem.*, **63**, 688 (2010).
[4] C. Metcalfe, J.A. Thomas. *Chem. Soc. Rev.*, **32**, 215 (2003).
[5] Y. Xiong, L.-N. Ji. *Coord. Chem. Rev.*, **185–186**, 711 (1999).
[6] P. Noblía, E.J. Baran, L. Otero, P. Draper, H. Cerecetto, M. González, O.E. Piro, E.E. Castellano, T. Inohara, Y. Adachi. Gambino. *Eur. J. Inorg. Chem.*, 322 (2004).
[7] K.H. Thompson, C. Orvig. *Coord. Chem. Rev.*, **219–221**, 1033 (2001).
[8] E.J. Baran. *J. Inorg. Biochem.*, **80**, 1 (2000).
[9] B.J. Hales, E.E. Case, J.E. Morningstar, M.R. Dzeda, L.A. Mauterer. *Biochemistry*, **25**, 7251 (1986).
[10] A. Messerschmidt, R. Wever. *Proc. Natl. Acad. Sci.*, **93**, 392 (1996).
[11] D.C. Crans, A.S. Tracey. *ACS Symposium Series*, Vol. 711, Chap. 2, American Chemical Society, Washington, DC (1998).
[12] R. Liasko, T.A. Kabanos, S. Karkabounas, M. Malamas, J.A. Tasiopoulos, D. Stefanou, P. Collery, A. Evangelou. *Anticancer Res.*, **18**, 3609 (1998).
[13] K.H. Thompson, J.H. McNeill, C. Orvig. *Chem. Rev.*, **99**, 2561 (1999).
[14] E.K. Efthimiadou, N. Katsaros, A. Karaliota, G. Psomas. *Bioorg. Med. Chem. Lett.*, **17**, 1238 (2007).
[15] P.K. Sasmal, A.K. Patra, A.R. Chakravarty. *J. Inorg. Biochem.*, **102**, 1463 (2008).
[16] A.A. El-Asmy, O.A. Al-Gammal, D.A. Saad, S.E. Ghazy. *J. Mol. Struct.*, **934**, 9 (2009).
[17] D. Kovala-Demertzi, M.A. Demertzis, J.R. Miller, C. Papadopoulou, C. Dodorou, G. Filousis. *J. Inorg. Biochem.*, **86**, 555 (2001).
[18] J. Marmur. *J. Mol. Biol.*, **3**, 208 (1961).
[19] M.E. Reichmann, S.A. Rice, C.A. Thomas, P. Doty. *J. Am. Chem. Soc.*, **76**, 3047 (1954).
[20] A. Wolfe, G.H. Shimer Jr, T. Meehan. *Biochemistry*, **26**, 6392 (1987).
[21] G. Cohen, H. Eisenberg. *Biopolymers*, **8**, 45 (1969).
[22] P. Noblía, M. Vieites, B.S. Parajón-Costa, E.J. Baran, H. Cerecetto, P. Draper, M. González, O.E. Piro, E.E. Castellano, A. Azqueta, A. López, A. Monge-Vega, D. Gambino. *J. Inorg. Biochem.*, **99**, 443 (2005).
[23] P. Noblía, E.J. Baran, L. Otero, P. Draper, H. Cerecetto, M. González, O.E. Piro, E.E. Castellano, T. Inohara, Y. Adachi, H. Sakurai, D. Gambino. *Eur. J. Inorg. Chem.*, 322 (2004).
[24] S.K.S. Hazari, J. Kopf, D. Palit, S. Rakshit, D. Rehder. *Inorg. Chim. Acta*, **362**, 1343 (2009).
[25] B. Khera, A.K. Sharma, N.K. Kaushik. *Polyhedron*, **2**, 1177 (1983).
[26] M. Tümer, H. Köksal, S. Serin, M. Digrak. *Transition Met. Chem.*, **24**, 13 (1998).
[27] M. Tümer, C. Çelik, H. Köksal, S. Serin. *Transition Met. Chem.*, **24**, 525 (1999).
[28] S.K. Dutta, S.B. Kumar, S. Bhattacharyya, E.R.T. Tiekink, M. Chaudhury. *Inorg. Chem.*, **36**, 4954 (1997).
[29] A.A. Nejo, G.A. Kolawole, A.R. Opoku, J. Wolowska, P. O'Brien. *Inorg. Chim. Acta*, **362**, 3993 (2009).
[30] R.L. Farmer, F.L. Urbach. *Inorg. Chem.*, **13**, 587 (1974).
[31] V.B. Arion, V.C. Kravtsov, R. Goddard, E. Bill, J.I. Gradinaru, N.V. Gerbeleu, V. Levitschi, H. Vezin, Y.A. Simonov, J. Lipkowski. *Inorg. Chim. Acta*, **317**, 33 (2001).
[32] A. Odani, R. Shimata, H. Masuda, O. Yamauchi. *Inorg. Chem.*, **30**, 2133 (1991).
[33] W. Qian, F. Gu, L. Gao, S. Feng, D. Yan, D. Liao, P. Cheng. *J. Chem. Soc., Dalton Trans.*, 1060 (2007).
[34] L.-N. Ji, X.-H. Zhou, J.-G. Liu. *Coord. Chem. Rev.*, **216–217**, 513 (2001).
[35] R.F. Pasternack, E.J. Gibbs, J.J. Villafranca. *Biochemistry*, **22**, 2406 (1983).
[36] C.V. Kumar, E.H. Asuncion. *J. Am. Chem. Soc.*, **115**, 8547 (1993).
[37] S. Satyanarayana, J.C. Dabroniak, J.B. Chaires. *Biochemistry*, **31**, 9319 (1992).
[38] R.J. Fiel, B.R. Munson. *Nucleic Acids Res.*, **8**, 2835 (1980).
[39] S. Satyanarayana, J.C. Daborusak, J.B. Chaires. *Biochemistry*, **32**, 2573 (1993).
[40] T. Uno, K. Hamasaki, M. Tannigawa, S. Shimabayashi. *Inorg. Chem.*, **36**, 1676 (1997).
[41] C.V. Kumar, E.H. Asuncion. *J. Am. Chem. Soc.*, **115**, 8547 (1993).
[42] J.M. Kelly, A.B. Tossi, D.J. McConnell, C. OhUigin. *Nucleic Acids Res.*, **13**, 6017 (1985).
[43] G.A. Neyhart, N. Grover, S.R. Smith, W.A. Kalsbeck, T.A. Fairley, M. Cory, H.H. Thorp. *J. Am. Chem. Soc.*, **115**, 4423 (1993).
[44] Z.P. Li, Y.H. Xing, Y.H. Zhang, G.H. Zhou, C.G. Wang, J. Li, X.Q. Zeng, M.F. Ge, S.Y. Niu. *J. Coord. Chem.*, **62**, 564 (2009).
[45] E.K. Efthimiadou, N. Katsaros, A. Karaliota, G. Psomas. *Bioorg. Med. Chem. Lett.*, **17**, 1238 (2007).
[46] J. Benítez, L. Guggeri, I. Tomaz, J.C. Pessoa, V. Moreno, J. Lorenzo. *J. Inorg. Biochem.*, **103**, 1386 (2009).